EurJOC

European Journal of Organic Chemistry

Chemistry Europe

European Chemical
Societies Publishing

Accepted Article

Title: Quantification of the Lewis Basicities and Nucleophilicities of 1,3,5-Tris(dialkylamino)benzenes

Authors: Gabriele Micheletti, Robert J. Mayer, Silvia Cino, Carla Boga, Andrea Mazzanti, Armin R Ofial, and Herbert Mayr

WILEY-VCH

FULL PAPER

Quantification of the Lewis Basicities and Nucleophilicities of 1,3,5-Tris(dialkylamino)benzenes

Gabriele Micheletti,[a] Robert J. Mayer,[b] Silvia Cino,[a] Carla Boga,*[a] Andrea Mazzanti,[a] Armin R. Ofial,[b] and Herbert Mayr*[b]

In memory of Professor Klaus Hafner, a great scientist and promoter of international collaborations

[a]   Dr. S. Cino, Dr. G. Micheletti, Prof. Dr. A. Mazzanti, Prof. Dr. C. Boga
        Department of Industrial Chemistry 'Toso Montanari'
        Alma Mater Studiorum – Università di Bologna
        Viale Risorgimento, 4 40136 Bologna (Italy)
        E-mail: carla.boga@unibo.it
        https://www.unibo.it/sitoweb/carla.boga/en
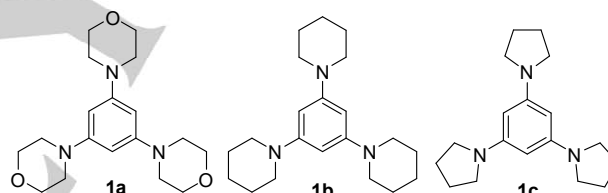[b]   Dr. R. J. Mayer, Dr. A. R. Ofial, Prof. Dr. H. Mayr
        Department Chemie
        Ludwig-Maximilians-Universität München
        Butenandtstr. 5–13, 81377 München (Germany)
        E-Mail: herbert.mayr@cup.uni-muenchen.de
        https://www.cup.uni-muenchen.de/oc/mayr/

        Supporting information for this article is given via a link at the end of the document.

Abstract: Equilibrium constants for the formation of Wheland complexes from 1,3,5-tris(dialkylamino)benzenes and benzhydrylium ions (Ar_2CH^+) have been determined photometrically in dichloromethane solution at 20 °C. The Lewis basicity of the ring carbons increases in the series trimorpholinobenzene < tripiperidinobenzene < tripyrrolidinobenzene. Wheland complexes which are formed with equilibrium constants $10^2 < K/M^{-1} < 10^6$ in the reactions of triaminobenzenes with carbenium ions show temperature-dependent dynamic ^1H NMR spectra, due to rapid reverse reactions and recombination at different positions of the Lewis bases. Since the rates of the formation of the Wheland complexes are too high to be measured directly, they were calculated as the product of photometrically determined equilibrium constants and the rate constants for the reverse reactions, which were derived from the dynamic ^1H NMR spectra. The experimentally determined equilibrium and rate constants were in good agreement with the results of DFT calculations using the SMD solvent model. The calculations show that in all cases the Wheland complexes are thermodynamically more stable than the ammonium ions formed by attack of the benzhydrylium ions at the amino group of the title compounds, which explains the exclusive formation of Wheland complexes in thermodynamically controlled reactions. With nucleophilicity parameters in the range $10 < N < 15$ the triaminobenzenes have comparable nucleophilic reactivities as enamines, silyl ketene acetals as well as stabilized phosphonium- and sulfonium ylides.

Scheme 1. 1,3,5-Tris(dialkylamino)benzenes **1**(**a-c**).

With oxidation potentials of $0.01 < E_{1/2}^{ox} < 0.35$ V vs Ag/Ag^+ in CH_3CN,[1] triaminobenzenes **1(a-c)** are strong reductants, comparable to the widely used sulfur-containing electron donor, tetrathiafulvalene.[2] The protonation of **1(a-c)**, which may occur at carbon or nitrogen, has carefully been investigated.[3] The Brønsted basicities of the carbon centers (pK_{aH} of 2.45 (**1a**), 4.64 (**1b**), and 9.62 (**1c**) in water[3]) are comparable to those of carboxylate ions. In line with these large pK_{aH} values, Wheland complexes obtained from the triaminobenzenes **1(a-c)** were isolated as persistent species at ambient temperature; their deprotonation requires treatment with bases, e.g. alkoxides.[1] The Boga group involved in this study has even isolated zwitterions from the reactions of the electron-rich triaminobenzenes **1** with electron deficient arenes (Scheme 2), thus linking the intermediates of electrophilic aromatic substitutions (Wheland complexes) with the intermediates of nucleophilic aromatic substitutions (Meisenheimer-Jackson complexes) in one molecule.[4]
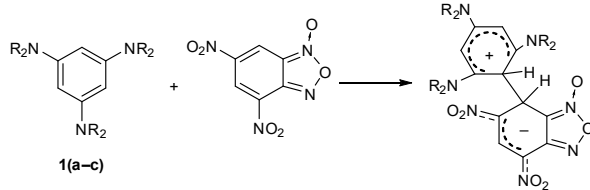
Introduction

Due to the strong electron-donating effect of dialkylamino groups, the 1,3,5-tris(dialkylamino)benzenes **1(a-c)** (Scheme 1) are compounds with exceptionally high electron density at the aromatic ring, which makes them valuable mechanistic tools for investigating general aspects of organic reactivity.

FULL PAPER

Scheme 2. Zwitterions from 1,3,5-tris(dialkylamino)benzenes **1(a-c)** and 4,6-dinitrobenzofuroxan.[4a]

Tris(dialkylamino)benzenes are ambident nucleophiles as well as Brønsted bases with two protonation sites, however, and the pK_{aH} values of the nitrogens has been reported to exceed that at carbon for **1a** (3.40) and **1b** (6.30), while the pyrrolidino derivate **1c** is mainly protonated at carbon ($K_{C/N}$ = 1600).

Anyway, the suitability of pK_{aH} values for predicting nucleophilic reactivities is known to be limited. As pointed out by Hine and Weimar, Brønsted correlations often suffer from the fact that pK_{aH} values refer to interactions with the proton, whereas the rate constants under consideration refer to interactions with another atom, *e.g.*, carbon, as in S_N2 reactions or Michael additions.[5] For that reason they suggested "carbon basicity", *i.e.*, relative affinities toward carbon centered Lewis acids, to replace Bronsted basicity (pK_{aH}) in analyses of rate-equilibrium relationships.[5] Recently, the Mayr group contributing to study has shown that para- and meta-substituted benzhydrylium ions (Ar_2CH^+) represent a family of Lewis acids which can be used as references for calibrating Lewis bases of widely variable strength and structure.[6] We now used the benzhydrylium ions **2(a-d)** not only to determine the Lewis basicities of **1(a-c)**, but also to quantify their nucleophilicities and thus provide parameters for rationalizing known and predicting new polar reactivities of the title compounds.[7] Since the differentiation of kinetic and thermodynamic quantities plays a crucial role in the following analyses, readers are reminded of the IUPAC recommendations to use the terms acidity and basicity for equilibrium constants and the terms electrophilicity and nucleophilicity for rate constants.[8]

Table 1. Benzhydrylium ions **2a–2d** (counterion: BF_4^-) used as reference compounds for quantifying the Lewis basicities and nucleophilicities of the triaminobenzenes **1(a-c)**.

Benzhydrylium Ions		Lewis Acidity LA[a]	Electro-philicity E[b]
	2a	-10.46	-7.69
	2b	-9.30	-7.02
	2c	-6.82	-5.53
	2d	-5.39	-3.85

[a] in CH_2Cl_2 ref.[6]; [b] ref.[7a]

Results and Discussion

Equilibrium constants for the reactions of triaminobenzenes 1 with benzhydrylium Ions 2.

The instant formation of the Wheland complexes **3xy** by reaction of the colorless triaminobenzenes **1** with the blue benzhydrylium tetrafluoroborates **2**-BF_4 (Scheme 3) is associated with a color change of the solution from blue to yellow-green. The structures of the resulting Wheland complexes (**3xy**) are derived from the NMR spectra presented in the next section.
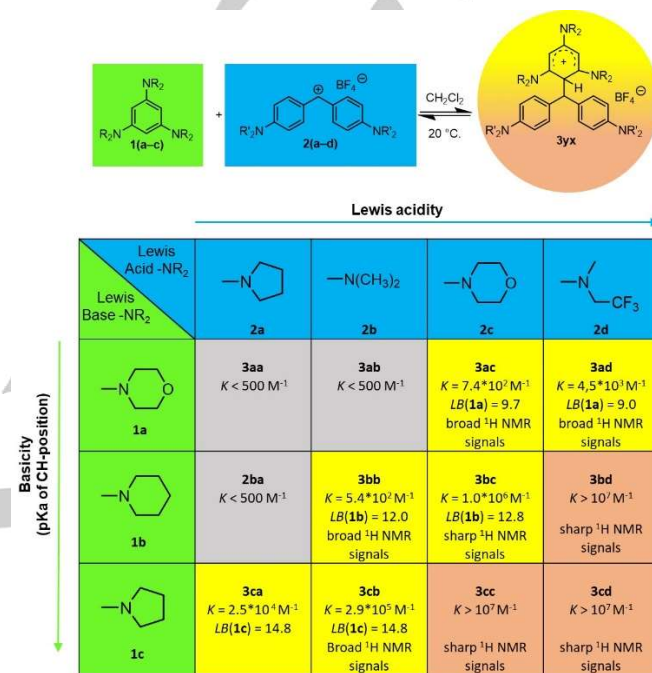
Scheme 3. Equilibrium constants determined by mixing 10^{-4} M solutions of triaminobenzenes **1** with equimolar amounts of benzhydrylium tetrafluoroborates (**2**-BF_4) and the resulting Lewis basicities (LB) in CH_2Cl_2. Green: triaminobenzenes; blue: benzhydrylium ions; gray: small equilibrium constants; yellow: intermediate equilibrium constants; orange: large equilibrium constants.

The equilibrium constants K of the association reactions of **1** with **2** (eq. 1) were determined by mixing equimolar amounts of the triaminobenzenes **1** and the benzhydrylium tetrafluoroborates **2**-BF_4^- in 10^{-4} M CH_2Cl_2 solution at 20 °C and measuring the absorbance of the blue benzhydrylium ions before ($[2]_0$) and after ($[2]_{eq}$) mixing with the aminobenzenes **1**.

$$K = \frac{\{[2]_0 - [2]_{eq}\}}{[2]_{eq}^2} \quad \text{(eq. 1)}$$

As specified in Table S1 and Scheme 3, the combination of the strongest Lewis base (**1c**) with **2c** and **2d**, as well as the reaction of **1b** with **2d** proceeded quantitatively or to such high degree of conversion that only lower limits of the corresponding equilibrium constants can be given (orange labeling in Scheme 3). On the other end, no or almost no consumption of the benzhydrylium ions was observed for the combination of the weakest Lewis base of this series (**1a**) with **2a** and **2b** and for the reaction of **1b** with **2a**, the weakest Lewis acid of this series; thus, only upper limits of the equilibrium constants can be derived for these combinations (grey

2

FULL PAPER

labeling in Scheme 3). For the remaining pairs (marked yellow in Scheme 3), which include combinations of the weak Lewis base **1a** with the strong Lewis acids **2c** and **2d** as well as the combinations of the strong Lewis base **1c** with the weak Lewis acids **2a** and **2b**, the equilibrium constants *K* listed in Scheme 3 could be determined.

In previous work, the Mayr group has demonstrated that equilibrium constants (CH₂Cl₂, 20 °C) for the reactions of benzhydrylium ions (and with lower precision also of other carbenium ions) with a variety of Lewis bases (pyridines, *tert*. amines, *tert*. phosphines, enamines, phenolate ions etc.) can be calculated by eq. 2, where *LA* is a Lewis acidity parameter and *LB* is a Lewis basicity parameter. The scales are anchored at $LA[(4\text{-MeOC}_6H_4)_2CH^+] = 0$.[6, 9, 10]

$$\log K(\text{CH}_2\text{Cl}_2, 20\ °C) = LA + LB; \qquad \text{(eq. 2)}$$

Insertion of the measured equilibrium constants (Table S1 and Scheme 3) and the Lewis acidities *LA* from Table 1 into eq. (2) yields the Lewis basicities *LB* (in CH₂Cl₂) of **1a** – **1c** shown in Scheme 3. The fact that the *LB* values for **1(a-c)** derived from equilibrium constants for the reactions with different benzhydrylium ions agree within one order of magnitude confirms the applicability of eq. (2).
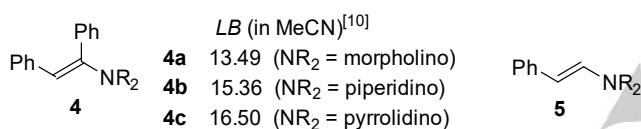

Figure 1. Structures of enamines **4** and **5**

A plot of the averaged Lewis basicities of the triaminobenzenes **1(a-c)** against the corresponding Lewis basicities of the enamines **4(a-c)**[10] (Figure 1) shows that in both series Lewis basicity increases in the order morpholino < piperidino < pyrrolidino (Figure 2). Since in the series **1a** – **1c** three amino groups are replaced, exchange of the NR₂ groups has a 1.8 times larger effect than in the enamine series **4a**–**4c**, where only one amino group is replaced. One cannot generalize this trend, however,

because experiments and calculations agree that piperidino and pyrrolidine substituted enamines **5** have almost equal Lewis basicity and nucleophilicity.[10]

As shown in Figure S63, the correlation of *LB*(**1a-1c**) with the corresponding pK_{aH} values in water[3b] has a slope of 0.77 with $R^2 = 0.94$.
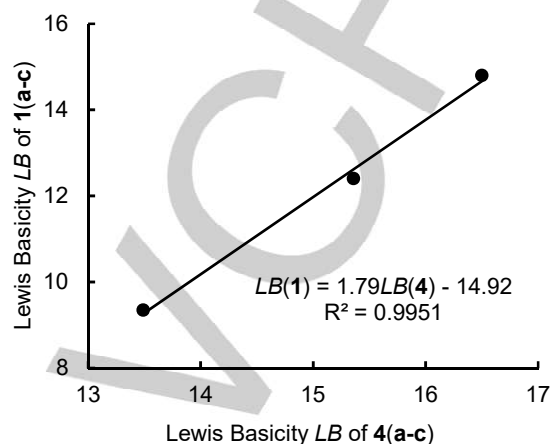

Figure 2. Plot of the Lewis basicities *LB* of the triaminobenzenes **1(a-c)** in CH₂Cl₂ against *LB* of the analogously substituted enamines **4(a-c)** in acetonitrile.

NMR-spectroscopic investigations of the reaction products 3xy.

Combinations of the triaminobenzenes **1b** and **1c** with the benzhydrylium ions **2c** and **2d**, *i. e.*, the four combinations located in the lower right square of Scheme 3 which are characterized by equilibrium constants $K \geq 10^6$ M^{-1}, gave rise to ¹H NMR spectra (400 MHz) with sharp lines in acetonitrile at 25 °C, as illustrated by the spectrum of **3cd** in Figure 3. The two doublets with *J* = 5.5 Hz for H-1 (δ = 4.12) and H-1' (δ = 4.34) corresponding to protons at sp³-hybridized carbons, are indicative for the formation of the Wheland complex **3cd**.

FULL PAPER

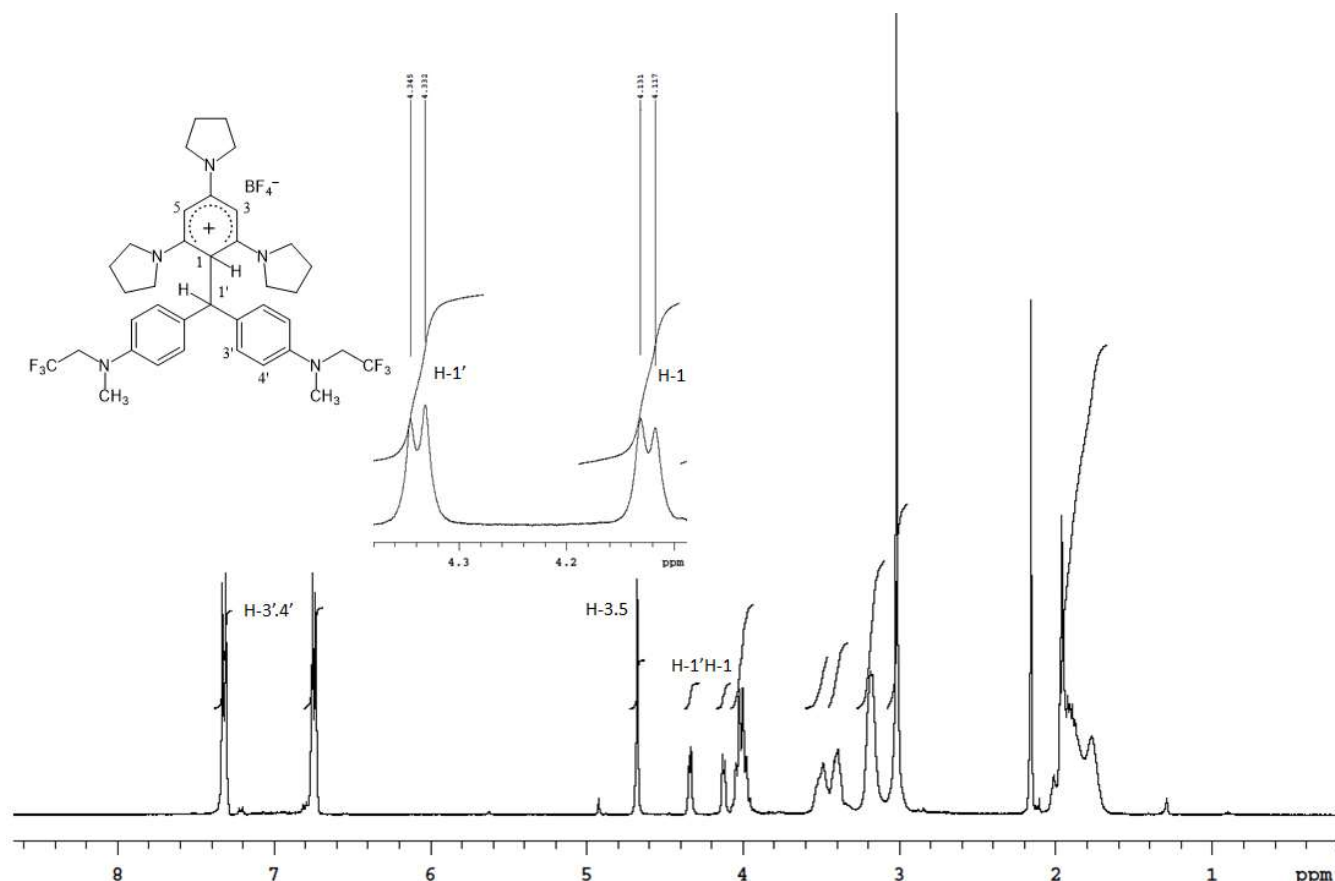**Figure 3.** ^{1}H NMR spectrum (400 MHz, CD$_3$CN, 25 °C) of Wheland complex **3cd** with expanded view for signals at δ = 4.34 and 4.12. NMR spectra in CD$_2$Cl$_2$ and CD$_3$CN are shown in the SI.

While **3bc** also showed a ^{1}H NMR spectrum with sharp signals at 25 °C, all other yellow-marked reaction products in Scheme 3 gave rise to broad ^{1}H NMR signals at ambient temperature, which sharpen when cooling down. For that reason, the NMR data listed in Table 2 have been collected at different temperatures.

The similarities of the ^{1}H and ^{13}C NMR chemical shifts in Table 2 confirm that all products observed by NMR have analogous structures **3xy**, and there is no evidence for the presence of products arising from N-attack at the aminobenzenes in any of these reactions. The reason for the regioselective C-attack of benzhydrylium ions, which contrasts the reactions with other electrophiles,[1,11] will be discussed below.

Table 2. Representative ^{1}H and ^{13}C NMR signals for Wheland complexes **3xy** in CD$_3$CN.[a]

	H-1, d (δ, J/Hz)	H-3,5, s (δ)	H-1', d (δ, J/Hz)	H-3', d (δ, J/Hz)	H-4', d (δ, J/Hz)	C-1 (δ)	C-3,5 (δ)	C-1' (δ)	C-3' (δ)	C-4' (δ)
3ac[b]	4.46, 5.8	5.32	4.22, 5.8	7.29, 8.9	6.89, 8.9	45.2	90.2	60.3	130.8	115.1
3ad[b]	4.45, 5.7	5.32	4.19, 5.7	7.25, 8.6	6.76, 8.6	45.5	90.1	60.4	130.8	112.0
3bb[b]	4.48, 4.9	5.30	4.17, 4.9	7.17, 8.5	6.62, 8.5	45.4	89.4	60.2	130.5	111.8

4

FULL PAPER

3bc[c]	4.53, 4.3	5.33	4.21, 4.3	7.25, 8.9	6.84, 8.9	46.2	90.5	61.4	131.2	115.5
3bd[c]	4.52, 4.5	5.34	4.19, 4.5	7.24, 8.7	6.76, 8.7	46.3	90.5	61.4	131.2	112.8
3cb[d]	4.07, 5.4	4.62	4.30, 5.4	7.26, 8.7	6.61, 8.7	51.2	87.8	58.0	130.7	111.9
3cc[c]	4.12, 5.3	4.67	4.35, 5.3	7.34, 8.3	6.82, 8.3	51.3	88.4	58.7	131.2	115.2
3cd[c]	4.12, 5.5	4.68	4.34, 5.5	7.32, 8.8	6.74, 8.8	51.5	88.5	58.7	131.3	112.6

[a] Assignment made by aid of *g*-COSY and *g*-HSQC experiments, all data in experimental, spectra in SI; [b] at -35 °C; [c] at 25 °C; [d]. at -14 °C.

As shown in Figure 4, the broad signals of **3bb** containing about 10 % of **2b** sharpen when cooling down, and at -30 °C one can additionally see the separate signals of **2b**, where the splitting of the aromatic hydrogens is due to hindered rotation of the aryl rings, as reported previously[12] (further details in SI, figures S52-S59). The dynamic process is reversible and the spectrum recorded on warming the sample to room temperature is identical to the starting one.
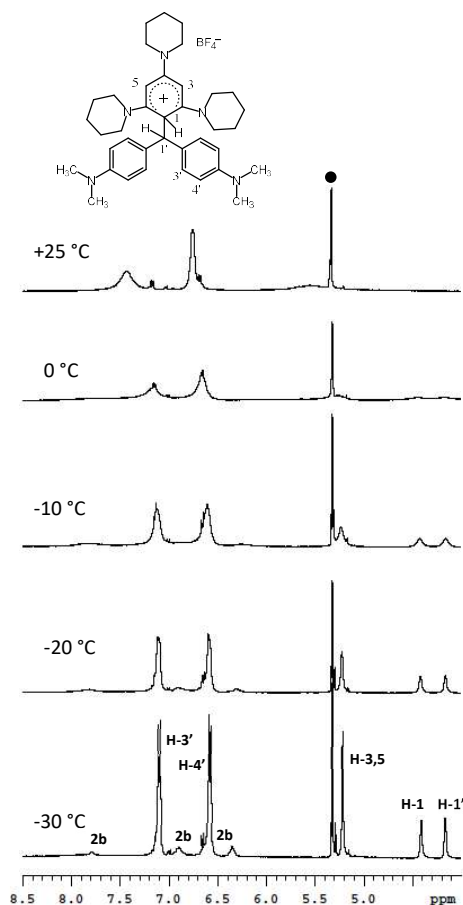

Figure 4. Variable temperature ¹H 600 MHz NMR spectra of **3bb** in CD₂Cl₂ in the presence of about 10% of **2b** (dot marks the solvent).

This behavior can be rationalized as follows: i) the cyclohexadienyl cation signals 1-H and 3,5-H of **3bb** exchange because of the heterolytic cleavage of **3bb** into **1b** and **2b** and subsequent recombination in a different position of the arene ring; ii) the "released" benzhydrylium ion **2b** can exchange with the excess **2b**.
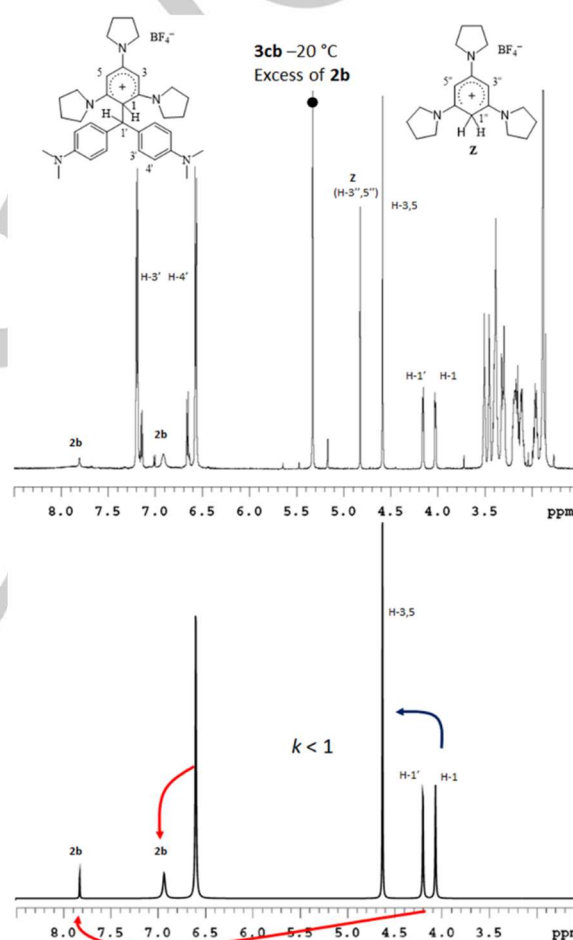

Figure 5. Top: ¹H NMR spectrum of **3cb** in CD₂Cl₂ at -20°C (with about 20% excess of **2b**). **Z** is protonated **1c**, probably derived by proton transfer from HBF₄ formed as by-product (see S30-S38); dot marks the solvent. Bottom: theoretical model for the simulation of dynamic exchange.

Analogous NMR experiments have been carried out on **3cb** in the presence of excess of **1c** or **2b**. The spectra at -20 °C in CD₂Cl₂ with about 20% excess of **2b** and related lineshape simulation are shown in Figure 5: the line at 4.0 ppm (H-1) coalesces with the line at 4.6 ppm (H-3,5) which can again be explained by heterolytic cleavage of **3cb** into reactants and recombination at

5

FULL PAPER

different positions of **1c** (H-1,3,5). The coalescence of the line at 4.15 ppm (H-1') with the line at 7.80 ppm and the coalescence of the line at 6.55 ppm with the line at 6.90 ppm is due to the exchange of the benzhydryl moiety of **3cb** with the "free" **2b**. When the VT NMR spectra of **3cb** were studied in the presence of **1c** (about 26%) a good simulation was obtained by considering the coalescence of H-1 and H-3,5 in the Wheland-complex **3cb** with the corresponding signals of free **1c** (Figure S47-S51). Under these conditions the NMR lines H-1', H-3', and H-4' remain sharp at any temperature, as experimentally observed.

Analogous reversible temperature-dependent sharpening and broadening of the ^{1}H NMR signals was observed for **3bb**, **3ac**, and **3ad**. All observations can be rationalized by the mechanism depicted in Scheme 4. Heterolytic cleavage of the Wheland complexes **3** regenerates the reactants triaminobenzene **1** and benzhydrylium ion **2**, which can recombine at the three equivalent positions CH-1, CH-3, and CH-5 and thus give rise to the coalescence of these three signals. If additional **1** or **2** is present, their NMR resonances are included in the exchange processes. Analogous dynamics have previously been observed for the Wheland complexes obtained by reaction of the triaminobenzenes **1** with superelectrophilic arenes, and can be illustrated as in Scheme 4.[4a,b]
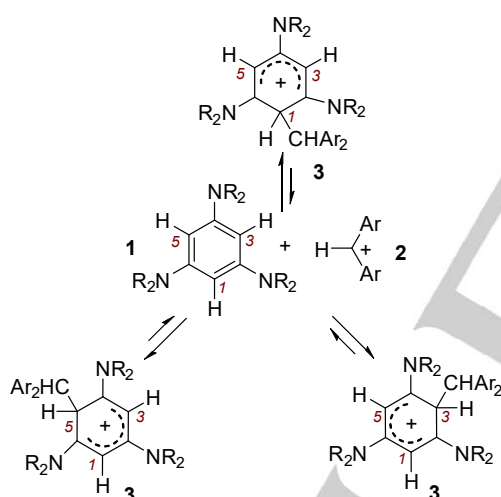
Scheme 4. Reversible formation of the Wheland complexes **3** accounts for the coalescence of H-1, H-3, H-5 and the exchange with added **1** or **2**.

As specified in the Supporting Information the Gibbs activation energies between -5 to 25 °C remain constant within experimental error, and the accuracy of our evaluations does not allow a separation into enthalpic and entropic contributions. Table 3 shows that the barriers for equilibration are slightly higher in acetonitrile than in dichloromethane.

Table 3. Barriers for equilibration ($\Delta G^{\ddagger}$/kJ mol^{-1} ± 1 at 20°C and 25 °C) of the ring protons of the cyclohexadienyl fragments of the Wheland complexes **3xy** determined by dynamic ^{1}H NMR spectroscopy.

Adduct	CD$_2$Cl$_2$ (20 °C)	CD$_2$Cl$_2$ (25 °C)	CD$_3$CN (20 °C)	CD$_3$CN (25 °C)
3ac			56.5	56.1
3ad	57.9	57.5	58.9	58.4
3bb	55.2	54.8	58.2	57.8
3cb	59.0	58.6	61.5	61.1

The reversible formation of the Wheland complexes suggested in Scheme 4 was confirmed by the substitution of the tripiperidinobenzene fragment in the Wheland complex **3bb** by the stronger Lewis base **1c**, as depicted in Scheme 5. Analogously, addition of **1c** to **3ad** produces formation of **3cd** and expulsion of **1a**; spectra are reported in S27-S29.
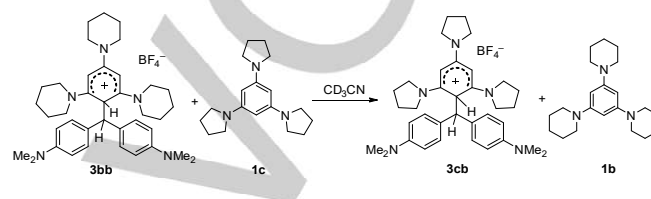
Scheme 5. Nucleophilic Substitution of the tripiperidinobenzene fragment in **3bb** by **1c** in acetonitrile at ambient temperature monitored by ^{1}H NMR spectroscopy.

Nucleophilicities of the triaminobenzenes 1(a-c).

In previous work, the Mayr group has developed the most comprehensive, presently available nucleophilicity scale,[7] including n-, π-, and σ-nucleophiles by measuring the rates of the reactions of the nucleophiles with a series of benzhydrylium ions **2** and structurally related quinone methides (reference compounds of known electrophilicity E). Plots of the measured second-order rate constants k (at 20 °C) against the corresponding E values give the nucleophile-specific susceptibilities s_N as the slopes, and the negative intercepts on the abscissa correspond to the solvent-dependent nucleophilicity parameters N, as defined by eq. 3.

$$\log k(20\,°C) = s_N(E + N); \qquad \text{(eq. 3)}$$

When trying to determine the nucleophilicities of the triaminobenzenes **1(a-c)** in this way, a problem was encountered. When tripiperidinobenzene **1b**, for example, was combined with benzhydrylium ion **2b**, almost no conversion was observed at the low concentrations required for the kinetic experiments. When **2b** was then replaced by the more reactive benzhydrylium ion **2c**, the reaction (**1b** + **2c**) was so fast (> 10^6 M^{-1}s^{-1}) that it could not be followed with stopped-flow techniques. The same problem arose when trying to measure the rates of the reactions of **1a** and **1c** with benzhydrylium ions: The reactions either did not take place because of missing thermodynamic driving force or were too fast for stopped-flow measurements. Analogous observations have previously been made when studying the reactions of benzhydrylium ions with nucleophiles which proceed via low Marcus intrinsic barriers.[13,14] This problem had been solved by using Laser flash spectroscopy where the benzhydrylium ions were generated with 7-ns laser pulses in the presence of nucleophiles.[13,14] In this way, the rates of reactions with low Marcus intrinsic barriers, which proceed with rate constants 10^6 <

6

FULL PAPER

$k < 10^{10}$ $M^{-1}s^{-1}$ could be measured. Since this method was not applicable here because of the UV absorptions of the aminobenzenes **1** around 250 nm, we approached the nucleophilic reactivities of **1(a-c)** differently.

In the preceding section we have shown that the temperature-dependence of the ^1H NMR spectra of the Wheland complexes **3xy** can be explained by the reversibility of their formation from the reactants **1** and **2**. The high degree of conversion of the reactants into the Wheland complexes **3xy** in the yellow and orange fields of Scheme 3 under the conditions of the NMR experiments implies that in these cases the forward reactions (electrophile-nucleophile combinations) are faster than the reverse reactions. For that reason, the barriers given for the equilibration of **3ac, 3ad, 3bb,** and **3cb** in Table 3 can be assigned to the activation Gibbs energies of the heterolytic cleavages. The similarity of the heterolysis rates measured in dichloromethane and acetonitrile is in accord with previous reports that S_N1 solvolysis rates of substrates with neutral leaving groups are not strongly affected by the solvent.[15]

The activation Gibbs energies in Table 3 can now be linked with the reaction Gibbs energies (derived from the equilibrium constants K in Scheme 3) to give the energies of the activated complexes relative to the reactants **1 + 2** as depicted in Scheme 6.
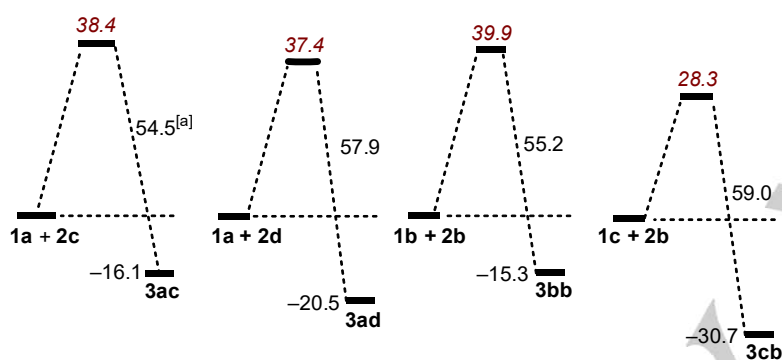
Scheme 6. Experimental reaction Gibbs energies (kJ/mol) for the reactions of the triaminobenzenes **1(a-c)** with benzhydrylium Ions **2** and activation Gibbs energies for the reverse reactions in CH_2Cl_2 at 20 °C. [a] Gibbs activation energy in CD_3CN (Table 3) reduced by 2 kJ mol^{-1}, the average difference between dichloromethane and acetonitrile.

The Eyring[16] equation was then used to convert the activation Gibbs energies for the reactions **1 + 2** shown in Scheme 6 into the corresponding rate constants listed in Table 4. Since it is not possible to determine rate constants for the reactions of each of the aminobenzenes **1(a-c)** with a series of benzhydrylium ions **2**, for the reasons discussed above, one cannot determine their susceptibilities s_N in the common way from lg k vs E plots, as described above. Approximate values of the nucleophilicity parameters N for **1a** -**1c** were, therefore, calculated by eq. (3) from lg$k$ (Table 4), the E-parameters of the benzhydrylium ions **2** (Table 1), and the assumption $s_N = 1$, a typical value for π_{CC}-nucleophiles.

Table 4. Rate constants for the reactions of triaminobenzenes **1** with benzhydrylium Ions **2** in dichloromethane at 20 °C ($M^{-1}s^{-1}$)[a]

Reaction	$k_\rightarrow$	log $k_\rightarrow$	N(**1**) for $s_N =1$
1a +2c	8.8×10^5	5.94	11.5
1a +2d	1.3×10^6	6.12	10.0
1b + 2b	4.7×10^5	5.68	12.7
1c + 2b	5.5×10^7	7.74	14.8

[a] From $\Delta G^{\#}$ in Scheme 6.

Trimorpholinobenzene **1a** is the only compound of this series for which N could be derived from two independent reactions (first two entries of Table 4). The deviation of the two values by 1.5 units of N is considered as an estimate of the error limit of this approach.

DFT Calculations

In order to examine our results by an independent method and elucidate the origin of the observed regioselectivities of these reactions (exclusive C-attack), DFT calculations at the MN15/def2-TZVP//MN15/def2-SVP level of theory using the SMD solvent model for dichloromethane have been performed for the reactions of the benzhydrylium ion **2b** with the triaminobenzenes **1(a-c)**. As shown in Table 5, the calculated reaction Gibbs energies ΔG^0 for the reactions with **1b** and **1c** agree with the experimental numbers within 6.5 kJ/mol, the calculated activation Gibbs energies $\Delta G^{\#}$ even within 2–5 kJ/mol. Our observation that **1a** does not react with **2b** is also in line with the calculated endergonicity for this reaction.

Table 5. Gibbs energies (kJ mol^{-1}) for the reaction of **2b** with triaminobenzenes **1(a-c)** at the SMD(CH_2Cl_2)/MN15/def2-TZVP//SMD(CH_2Cl_2)/MN15/def2-SVP level of theory.

	1a	**1b**	**1c**
$\Delta G^{\ddagger}$ (C-C)	+62.2(Exp: no rxn)	+44.3(Exp: 39.9)	+25.9 (Exp: 28.3)

7

FULL PAPER

ΔG^0 (C-C)	+9.8 (Exp: no rxn)	-9.4 (Exp: -15.3)	-24.2 (Exp: -30.7)

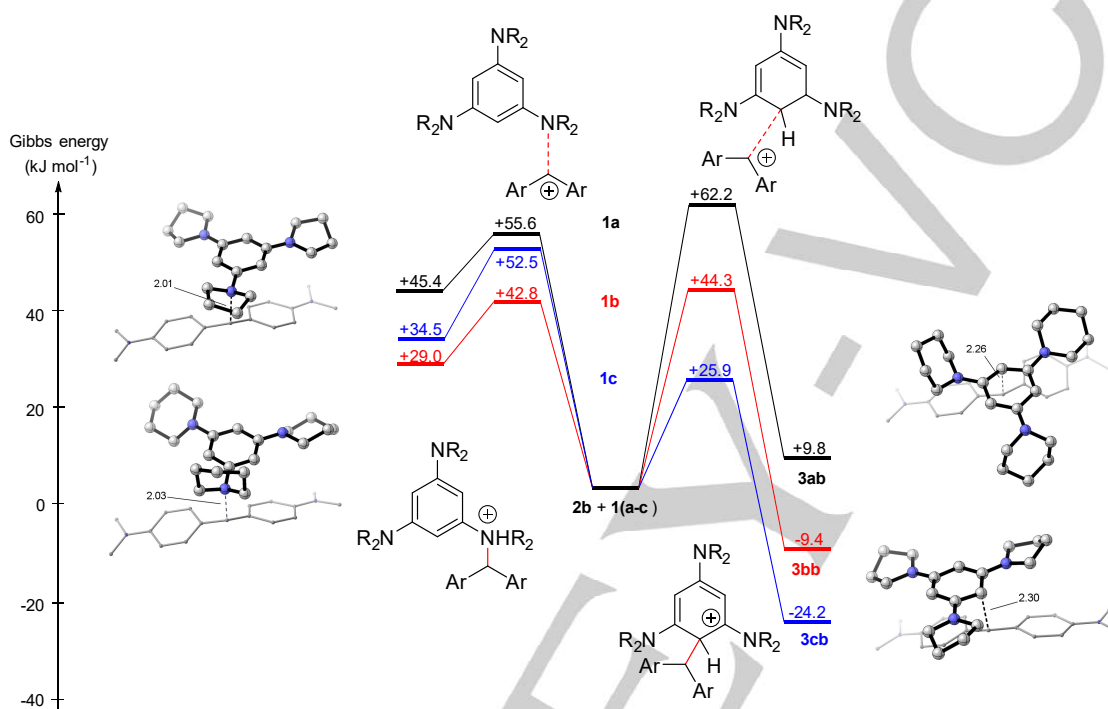| $\Delta G^{\ddagger}$ (C-N)	+55.6	+42.8	+52.5
ΔG^0 (C-N)	+45.4	+29.0	+34.5

Figure 6. Gibbs energy profile for the reaction of benzhydrylium ion **2b** with triaminobenzenes **1a** -**1c** at the SMD(CH$_2$Cl$_2$)/MN15/def2-TZVP//SMD(CH$_2$Cl$_2$)/MN15/def2-SVP level of theory.

Figure 6 not only reveals why **2b** does not react with **1a** under conditions where the resulting Wheland complexes are not deprotonated, but also explains why products of N-attack have not been observed in any of the reactions investigated during this work. All benzhydryl-substituted ammonium ions (left part of Figure 6) are thermodynamically much less stable than the corresponding Wheland complexes **3**, and even if N-attack is faster than C-attack, which might be the case in the reaction of **2b** with the piperidino compound **1b**, the barrier for retroaddition is so low that rearrangement of the initially formed quaternary ammonium ion into the Wheland complex **3bb** would occur immediately.

In line with our experimental findings, the increasing thermodynamic stability of the Wheland complexes in the series morpholino < piperidino < pyrrolidino (**3ab** < **3bb** < **3cb**) is accompanied by decreasing activation Gibbs energies $\Delta G^{\#}$ (morpholino > piperidino > pyrrolidine) for their formation.

The ordering is different for N-alkylation. Now, attack at the piperidino nitrogen of **1b** is faster and thermodynamically more favorable than N-attack at the pyrrolidine ring of **1c**, because in the latter case resonance stabilization of the pyrrolidine nitrogen

through the aromatic ring has to be abandoned. By this effect, C-attack at **1c** is favored while N-attack is disfavored compared with the corresponding reactions of **1b**.

Though the relative activation energies for C- and N-attack in Figure 6 are not perfectly transferrable to S$_N$2 type reactions, they represent a frame to rationalize the previously reported regioselectivities of the reactions of **1(a-c)** with alkylating agents. In line with the lower barrier for C-attack at tripyrrolidinobenzene **1c** in Figure 6, Effenberger reported that the kinetically controlled reactions of **1c** with alkyl halides in dimethoxyethane resulted in the exclusive formation of C-alkylated products.[17a] Analogous reactions of **1c** with alkyl halides in ethanol resulted in the predominant (> 70 %) or exclusive formation of C-alkylated products.[17b] The opposite regioselectivity, *i.e.,* exclusive *N*-methylation has been observed in the reaction of tripiperidinobenzene **1b** with methyl iodide in DMSO,[18] in accord with the lower barrier for *N*-attack shown in Figure 6.

While alkylations which undergo irreversible reactions with **1a-1c** thus give products of C- or N-attack, only products of C-attack are formed in thermodynamically controlled reactions of the triaminobenzenes **1** with C-electrophiles. The exclusive formation

8

FULL PAPER

of Wheland complexes **3**, which was observed in the reversible reactions of 4,6-dinitrobenzofuroxan ($E = -5.06$)[19] with **1a-1c** (Scheme 2),[4a] is in line with Figure 6, showing that in all cases the Wheland complexes are more stable than the ammonium ions arising from N-attack.

Conclusion

The Wheland complexes **3xy**, formed by C-attack of benzhydrylium ions at the triaminobenzenes **1(a-c)** are thermodynamically more stable than the isomeric ammonium ions formed by attack at the nitrogen of **1(a-c)**. It can, therefore, be expected that all C-electrophiles which undergo reversible reactions with **1(a-c)** will give products of C-attack. Since the activation energies for N- and C-attack do not differ strongly, kinetically controlled alkylations of the triaminobenzenes **1(a-c)** may occur either at carbon (preferred for **1c**) or at nitrogen (preferred for **1a,b**).

From the photometrically measured equilibrium constants for the reactions of **1(a-c)** with the benzhydrylium ions **2(a-d)**, Lewis basicity parameters *LB* have been determined for the triaminobenzenes **1**, which can be linked with previously published Lewis acidities *LA* of carbon-centered electrophiles (carbenium ions) to predict the thermodynamic stabilities of the resulting Wheland complexes.

Wheland complexes **3xy**, which are formed with small equilibrium constants, show dynamic ^{1}H NMR spectra due to heterolytic cleavage and recombination of the fragments. The activation Gibbs energies of these processes reflect the rates of the heterolytic cleavages. Linkage of these $\Delta G^{\neq}$ values with the reaction Gibbs energies for Wheland complex formation give the activation Gibbs energies for the reactions of the triaminobenzenes with the benzhydrylium ions (Scheme 6) from which rough values for the nucleophilicity parameters N of **1(a-c)** have been derived. Scheme 7 shows that the activation of the benzene ring through the three amino groups is so strong that the title compounds have nucleophilicities comparable to enamines, alkyl-activated pyrroles, silyl ketene acetals, diazoalkanes, and acceptor substituted sulfur- and phosphorous ylides, though electrophilic C-attack at **1(a-c)** is associated with destruction of aromaticity.
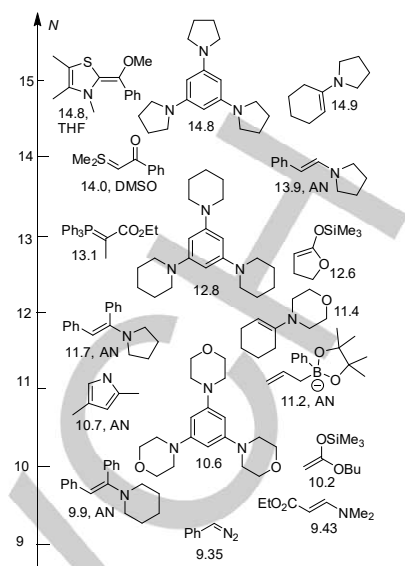
Scheme 7. Comparison of the nucleophilicities *N* (assumption $s_N = 1$) of the triaminobenzenes **1(a-c)** with those of other C-centered nucleophiles.

Experimental Section

Experimental Details. The NMR experiments (^{1}H-, ^{13}C-, DEPT, *g*-COSY, *g*-HSQC, and variable–temperature) were recorded on Mercury 400 or Inova 600 (Varian, Palo Alto USA) spectrometers operating at 400 or 600 MHz (for ^{1}H NMR) and 100.56 or 150.80 MHz (for ^{13}C NMR), respectively. Chemical shifts were measured in δ (ppm) with reference to the solvent [for ^{1}H and ^{13}C NMR, respectively: δ = 5.30 and 54.2 for CD$_2$Cl$_2$; δ = 7.26 and 77.0 for CDCl$_3$; δ = 1.96 and 118.1 for CD$_3$CN]. *J* values are given in Hz. The low-temperature NMR spectra were obtained by using a flow of dry nitrogen which entered into an inox steel heat exchanger immersed in liquid nitrogen and connected to the NMR probe head by a vacuum-insulated transfer line. The 600 MHz ^{1}H NMR spectra were acquired using a 5 mm direct probe. Temperature calibrations were performed before the experiments, using a digital thermometer and a Cu/Ni thermocouple placed in an NMR tube filled with isopentane or 1,1,2,2-tetrachloroethane (for the low and high temperature range, respectively). The uncertainty in the temperature measurements can be estimated from the calibration curve as ±1 °C. Line shape simulations were performed using a PC version of the QCPE DNMR6 program.[20] A copy of the program is available on request from the authors (A.M.). Electronic superimposition of the original and the simulated spectra enabled the determination of the most reliable rate constants at a few different temperatures. These constants provided the free energies of activation ($\Delta G^{\neq}$) by means of the Eyring equation.[16] UV/Vis spectra were recorded on a PerkinElmer Lambda 12 spectrophotometer, at 20 °C in CH$_2$Cl$_2$ and in quartz cells (path length cell: 0.1 cm). More details are reported in Table S1. Solvents and reagents were commercial materials (Aldrich or Fluka) if not specified. CH$_2$Cl$_2$ for spectrophotometric measurements was freshly distilled over P$_2$O$_5$. Triaminobenzenes **1(a-c)** were obtained as reported previously.[4a] Benzhydrylium tetrafluoroborates **2a-d** were prepared as described previously.[21]

Formation of 3xy. General procedure. [22] The triaminobenzene derivative **1a** (or **1b**, or **1c**, 0.02 mmol) was weighed directly into the NMR spectroscopy tube and dissolved in the minimum amount of solvent (CD$_3$CN or CD$_2$Cl$_2$). Then, an equivalent of the benzhydrylium tetrafluoroborate **2b** (or **2c**, or **2d**) dissolved in the solvent was added (usually, the total amount of deuterated solvent used was 1 mL).

9

FULL PAPER

Immediately after the mixing of the reagents, the ^{1}H NMR spectrum was recorded and for combinations **1b/2d**, **1c/2d**, **1b/2c**, and **1c/2c**, the ^{1}H NMR spectrum of the reaction mixture recorded at 25°C showed disappearance of the signals of the reagents and appearance of sharp signals due to the quantitative formation of **3bd**, **3cd**, **3bc**, and **3cc**, respectively. The ^{1}H NMR spectrum recorded at 25 °C for combinations **1a/2d**, **1a/2c**, **1b/2b**, and **1c/2b** showed very broad signals. These reactions were carried out at low temperature: the nucleophile solution was first introduced in the NMR spectroscopy tube that was inserted in the NMR probe. When the probe temperature reached −80°C for the reactions carried out in CD$_2$Cl$_2$, or −35°C for those in acetonitrile, the NMR tube was quickly removed and an equivalent of benzhydrylium compound **2** was added. Immediate formation of **3ad**, **3ac**, **3bb**, or **3cb** was confirmed by the appearance of the typical signals in the ^{1}H-NMR spectrum. The system was monitored over time and at different temperatures until 25 °C.

4-(4-(bis(4-morpholinophenyl)methyl)-3,5-dimorpholinocyclohexa-2,5-dien-1-ylidene)morpholin-4-ium tetrafluoroborate (3ac): ^{1}H NMR (600 MHz, CD$_3$CN, -35 °C): δ = 7.29 (d, J = 8.9 Hz, 4 H), 6.89 (d, J = 8.9 Hz, 4 H), 5.32 (s, 2 H), 4.46 (d, J = 5.8 Hz, 1 H), 4.22 (d, J = 5.8 Hz, 1 H), 3.78 (t, J = 4.5, 8 H), 3.86-3.62 (m, 8 H), 3.60-3.37 (m, 8 H), 3.34-3.16 (m, 8 H), 3.15-3.06 ppm (m, 8 H); ^{13}C NMR (150.80 MHz, CD$_3$CN, -35 °C): δ = 164.8 (C), 162.6 (C), 150.2 (br.s., C), 130.8 (br.s., CH), 129.9 (br.s., C), 115.1 (br.s., CH), 90.2 (CH), 66.5 (OCH$_2$), 66.3 (OCH$_2$), 65.9 (br.s. OCH$_2$), 65.6 (br.s. OCH$_2$), 60.3 (CH), 49.2 (br.s., NCH$_2$), 48.0 (NCH$_2$), 47.9 (NCH$_2$), 45.2 ppm (CH).

4-(4-(bis(4-(methyl(2,2,2-trifluoroethyl)amino)phenyl)methyl)-3,5-dimorpholinocyclohexa-2,5-dien-1-ylidene)morpholin-4-ium tetrafluoroborate (3ad): ^{1}H NMR (600 MHz, CD$_3$CN, -35 °C): δ = 7.25 (d, J = 8.6 Hz, 4 H), 6.76 (d, J = 8.6 Hz, 4 H), 5.32 (s, 2 H), 4.45 (d, J = 5.7 Hz, 1 H), 4.19 (d, J = 5.7 Hz, 1 H), 4.11-3.95 (m, 4 H), 3.85-3.57 (m, 8 H), 3.54-3.40 (m, 8 H), 3.32-3.19 (m, 8 H), 3.02 ppm (s, 6H); ^{13}C NMR (150.80 MHz, CD$_3$CN, -35 °C): δ = 165.0 (C), 162.8 (C), 147.8 (C), 130.8 (CH), 127.2 (C), 126.5 (q, J_{C-F}= 285.0 Hz, CF$_3$), 112.0 (CH), 90.1 (CH), 66.5 (CH$_2$), 65.7 (CH$_2$), 60.4 (CH), 52.7 (q, J_{C-F} = 32.3 Hz, CH$_2$CF$_3$), 48.0 (CH$_2$), 45.5 (CH), 40.9 (CH$_2$), 39.0 ppm (CH$_3$); ^{1}H NMR (600 MHz, CD$_2$Cl$_2$, -80 °C): δ = 7.13 (d, J = 8.3 Hz, 4 H), 6.64 (d, J = 8.3 Hz, 4 H), 5.24 (s, 2 H), 4.46 (d, J = 3.3 Hz, 1 H), 4.05 (d, J = 3.3 Hz, 1 H), 3.98-3.51 (m, 16 H), 3.44-3.05 (m, 12 H), 2.95 ppm (s, 6 H); ^{13}C NMR (150.80 MHz, CD$_2$Cl$_2$, -80 °C): δ = 164.8 (C), 161.1(C), 146.7(C), 129.7(CH), 125.2(C), 125.1 (q, J_{C-F} = 283.5 Hz, CF$_3$), 111.0 (CH), 89.0 (CH), 66.0 (CH$_2$), 65.6 (CH$_2$), 64.8(CH$_2$), 60.8 (CH), 52.6 (q, J_{C-F} = 33.8 Hz, CF$_3$), 48.1 (CH$_2$), 47.1 (CH$_2$), 46.7 (CH$_2$), 44.8 (CH), 39.8 ppm (CH$_3$).

1-(4-(bis(4-(dimethylamino)phenyl)methyl)-3,5-di(piperidin-1-yl)cyclohexa-2,5-dien-1-ylidene)piperidin-1-ium tetrafluoroborate (3bb): ^{1}H NMR (600 MHz, CD$_3$CN, -30 °C): δ = 7.17 (d, J=8.5 Hz, 4 H), 6.62 (d, J=8.5 Hz, 4 H), 5.30 (s, 2 H), 4.48 (d, J=4.9 Hz, 1 H), 4.17 (d, J=4.9 Hz, 1 H), 3.45 (t, J=4.9 Hz, 4 H), 3.27-3.12 (m, 8 H), 2.87 (s, 12 H), 1.76-1.42 ppm (m, 18 H); ^{13}C NMR (150.80 MHz, CD$_3$CN, -35 °C): δ = 163.3 (C), 162.0 (C), 149.7 (C), 130.5 (CH), 127.7 (C), 111.8 (CH), 89.4 (CH), 60.2 (CH), 49.6 (br.s, NCH$_2$), 49.1 (NCH$_2$), 45.4 (CH), 40.0 (CH$_3$), 26.6 (NCH$_2$CH$_2$), 25.0 (NCH$_2$CH$_2$), 24.2 (NCH$_2$CH$_2$CH$_2$), 23.3 ppm (NCH$_2$CH$_2$CH$_2$); ^{1}H NMR: (600 MHz, CD$_2$Cl$_2$, -80 °C): δ = 7.05 (d, J = 8.8 Hz, 4 H), 6.52 (d, J = 8.8 Hz, 4 H), 5.17 (s, 2H), 4.37 (d, J = 4.0 Hz, 1 H), 4.16 (d, J = 4.0 Hz, 1 H), 3.74-2.96 (m.s, 12 H), 2.83 (s, 12 H), 1.70-1.04 ppm (m, 18 H); ^{13}C NMR (150.80 MHz, CD$_2$Cl$_2$, -80 °C): δ = 161.6 (C), 160.3 (C), 148.7 (C), 129.9 (CH), 123.9 (C), 111.1 (CH), 88.8 (CH), 59.3 (CH), 49.6 (NCH$_2$), 49.0 (NCH$_2$), 48.4 (NCH$_2$), 45.1 (CH), 40.2 (CH$_3$), 26.3 (NCH$_2$CH$_2$), 25.9 (NCH$_2$CH$_2$), 24.5 (CH$_2$), 23.9 (CH$_2$), 23.8 ppm (CH$_2$).

1-(4-(bis(4-morpholinophenyl)methyl)-3,5-di(piperidin-1-yl)cyclohexa-2,5-dien-1-ylidene)piperidin-1-ium tetrafluoroborate (3bc): ^{1}H NMR (400 MHz, CD$_3$CN, 25 °C): δ = 7.25 (d, J = 8.9 Hz, 4 H), 6.84 (d, J = 8.9 Hz, 4 H), 5.33 (s, 2 H), 4.53 (d, J = 4.3 Hz, 1 H), 4.21 (d, J = 4.3 Hz, 1 H), 3.80 (t, J = 4.2 Hz, 8 H), 3.70 (t, J = 3.7 Hz, 8 H), 3.48 (t, J = 5.6 Hz, 4 H), 3.26 (t, J = 4.6 Hz, 8 H), 1.76-1.42 ppm (m, 18 H); ^{13}C NMR

(100.56 MHz, CD$_3$CN, 25 °C): δ = 164.7 (C), 164.5 (C), 151.4 (C), 131.2 (br. CH), 130.2 (br.s, C), 115.5 (CH), 90.5 (CH), 67.23 (OCH$_2$), 67.18 (OCH$_2$), 61.4 (CH), 50.3 (br.s., NCH$_2$), 50.1 (br.s., NCH$_2$), 50.0 (br.s., NCH$_2$), 49.7 (br.s., NCH$_2$), 46.2 (CH), 27.0 (br s., NCH$_2$CH$_2$), 26.2 (br s., NCH$_2$CH$_2$), 24.6 (br.s., NCH$_2$CH$_2$CH$_2$), 24.5 ppm (br s., NCH$_2$CH$_2$CH$_2$).

1-(4-(bis(4-(methyl(2,2,2-trifluoroethyl)amino)phenyl)methyl)-3,5-di(piperidin-1-yl)cyclohexa-2,5-dien-1-ylidene)piperidin-1-ium tetrafluoroborate (3bd): ^{1}H NMR (400 MHz, CD$_3$CN, 25 °C): δ = 7.24 (d, J=8.7 Hz, 4 H), 6.76 (d, J=8.7 Hz, 4 H), 5.34 (s, 2 H), 4.52 (d, J=4.5 Hz, 1 H), 4.19 (d, J=4.5 Hz, 1 H), 4.00 (q, J=9.4 Hz, 4 H), 3.60-3.40 (m, 4 H), 3.25 (t, J= 5.4 Hz, 8 H), 3.02 (s, 6 H), 1.73-1.62 (m, 4 H), 1.62-1.55 (m, 6 H), 1.55-1.45 ppm (m, 8 H); ^{13}C NMR (100.56 MHz, CD$_3$CN, 25 °C): δ = 164.8 (C), 163.2 (C), 148.6 (C), 131.2 (CH), 127.9 (C), 127.0 (q, J = 283 Hz, CF$_3$), 112.8 (CH), 90.5 (CH) , 61.4 (CH), 53.7 (q, J = 31.7 Hz, CF$_3$), 50.1 (CH$_2$), 49.7 (CH$_2$), 48.5 (CH$_2$), 46.3 (CH) 39.5 (CH$_3$), 26.94 (CH$_2$), 26.86 (CH$_2$), 26.1 (CH$_2$), 24.6 ppm (CH$_2$); ^{1}H NMR (400 MHz, CD$_2$Cl$_2$, -85 °C): δ = 7.07 (d, J=8.6 Hz, 4H), 6.61 (d, J=8.6 Hz, 4H), 5.17 (s, 2H), 4.39 (d, J=3.5 Hz, 1 H), 4.18 (d, J=3.5 Hz, 1 H), 3.84 (q, J=8.2 Hz, 4 H), 3.74-3.60 (m$_s$, 2 H), 3.33-2.88 (m$_s$, 10 H), 2.93 (s, 6H), 1.71-1.34 (m, 14 H), 1.29-1.14 (m, 2 H), 1.14-0.96 ppm (m, 2 H).

1-(4-(bis(4-(dimethylamino)phenyl)methyl)-3,5-di(pyrrolidin-1-yl)cyclohexa-2,5-dien-1-ylidene)pyrrolidin-1-ium tetrafluoroborate (3cb): ^{1}H NMR (600 MHz, CD$_3$CN, -14 °C): δ = 7.26 (d, J = 8.7 Hz, 4 H), 6.61 (d, J = 8.7 Hz, 4 H), 4.62 (s, 2 H), 4.30 (d, J = 5.4 Hz, 1 H), 4.07 (d, J = 5.4 Hz, 1 H), 3.53-2.80 (m.s, 12 H) 2.86 (s, 12 H), 1.95-1.78 (m, 8 H), 1.78-1.67 ppm (m, 4 H); ^{13}C NMR (150.80 MHz, CD$_3$CN, -14 °C): δ = 160.8 (C), 160.4 (C), 150.3 (C), 130.7 (CH), 128.0 (C), 111.9 (CH), 87.8 (CH), 58.0 (CH), 51.2 (CH), 49.04 (NCH$_2$), 48.98 (NCH$_2$), 48.89 (NCH$_2$), 40.2 (CH$_3$), 25.7 (NCH$_2$CH$_2$), 25.1 (NCH$_2$CH$_2$), 24.8 ppm (NCH$_2$CH$_2$); ^{1}H NMR (600 MHz, CD$_2$Cl$_2$, -80 °C): δ = 7.12 (d, J = 8.4 Hz, 4 H), 6.49 (d, J = 8.4 Hz, 4 H), 4.48 (s, 2 H), 4.09 (d, J = 5.0 Hz, 1 H), 3.94 (d, J = 5.0 Hz, 1 H), 3.50-3.00 (m.s, 12 H), 2.82 (s, 12 H), 1.97-1.60 ppm (m, 12 H); ^{13}C NMR (150.80 MHz, CD$_2$Cl$_2$, -20 °C): (CH$_2$ signals tentatively assigned, see fig. S22) δ = 160.8 (C), 160.4 (C), 150.2 (C), 130.5 (CH), 128.2 (C), 111.8 (CH), 87.6 (CH), 59.7 (CH), 51.7 (CH), 49.4 (NCH$_2$), 49.3 (NCH$_2$), 40.8 (CH$_3$), 26.0 (NCH$_2$CH$_2$), 25.8 ppm (NCH$_2$CH$_2$).

1-(4-(bis(4-morpholinophenyl)methyl)-3,5-di(pyrrolidin-1-yl)cyclohexa-2,5-dien-1-ylidene)pyrrolidin-1-ium tetrafluoroborate (3cc): ^{1}H-NMR (600 MHz, CD$_3$CN, 25 °C): δ = 7.34 (d, J=8.3 Hz, 4 H), 6.82 (d, J = 8.3 Hz, 4 H), 4.67 (s, 2 H), 4.35 (d, J = 5.3 Hz, 1 H), 4.12 (d, J = 5.3 Hz, 1 H), 3.78 (t, J = 4.8, 8 H), 3.56-3.30 (m, 8 H), 3.22-3.13 (m, 4 H), 3.09 (t, J = 4.8, 8 H), 2.01 (br.s, 4 H), 1.95-1.68 ppm (m, 8 H); ^{13}C NMR (150.80 MHz, CD$_3$CN, 25 °C): δ = 161.4 (C), 161.1 (C), 151.6 (C), 131.2 (CH), 130.5 (C), 115.2 (CH), 88.4 (CH), 67.2 (OCH$_2$), 67.17 (OCH$_2$), 58.7 (CH), 51.3 (CH), 50.1 (NCH$_2$), 49.7 (NCH$_2$), 49.54 (NCH$_2$), 49.47 (NCH$_2$), 25.43 (NCH$_2$CH$_2$), 25.38 ppm (NCH$_2$CH$_2$).

1-(4-(bis(4-(methyl(2,2,2-trifluoroethyl)amino)phenyl)methyl)-3,5-di(pyrrolidin-1-yl)cyclohexa-2,5-dien-1-ylidene)pyrrolidin-1-ium tetrafluoroborate (3cd): ^{1}H NMR (400 MHz, CD$_3$CN, 25 °C): δ = 7.32 (d, J=8.8 Hz, 4 H), 6.74 (d, J=8.8 Hz, 4 H), 4.68 (s, 2 H), 4.34 (d, J=5.5 Hz, 1 H), 4.12 (d, J=5.5 Hz, 1 H), 4.01 (q, J=9.6 Hz, 4 H), 3.57-3.44 (m, 2 H), 3.44-3.35 (m, 2 H), 3.25-3.11 (m, 6 H), 3.11-2.90 (m, 2 H), 3.02 (s, 6 H), 1.93-1.67 ppm (m, 12 H); ^{13}C NMR (100.56 MHz, CD$_3$CN, 25 °C): δ = 161.4 (C), 161.3 (C), 148.7(C), 131.3(CH), 129.0(C), 126.5 (q, J_{C-F} = 283.1 Hz, CF$_3$), 112.6 (CH), 88.5 (CH), 58.7 (CH), 53.7 (q, J_{C-F} = 31.9 Hz, CF$_3$), 51.5 (CH), 49.55 (CH$_2$), 49.5 (CH$_2$), 39.6 (CH$_3$), 26.0 (CH$_2$), 25.1 ppm (CH$_2$).

Exchange of the nucleophilic moiety. To a CD$_3$CN solution of **1b** (2.0x10^{-5} mol in 0.7 mL) an equivalent of **2b** was added and the resulting ^{1}H NMR spectrum of **3bb** was recorded. Then, an equimolar amount of **1c** was added. Immediately after mixing, the ^{1}H NMR spectrum showed disappearance of signals ascribed to the piperidinyl moiety in **3bb** and concomitant appearance of signals belonging to the Wheland complex **3cb**

10

10.1002/ejoc.202100939

FULL PAPER

together with typical signals for the free nucleophile **1b** (spectra in Figure S-25). Analogous behavior was observed for the reaction between **1a** and **2d**; in this case the ^{1}H NMR spectrum showed, after addition of an equimolar amount of **1c**, formation of **3cd** and signals of **1a** (spectra in Figure S-26). This latter reaction was carried out also at –20 °C, in this case the mixing of **1a** with **2d** produced an orange/yellow solution which ^{1}H NMR spectrum showed well resolved signals belonging to **3ad**; addition of one equivalent of **1c** produced disappearance of signals of **3ad** and concomitant appearance of those of **3cd** and of **1a** (spectra in Figure S-27).

DFT calculated Gibbs energy profile for the reaction of 2b with triaminobenzenes

Initially, all structures were subjected to a conformational search using the OPLS3[23] force field as implemented in Macromodel.[24] A set of the lowest conformers was then optimized with the Gaussian 16 software package[25] at the SMD(DCM)[26]/MN15[27]/def2-SVP[28] level of theory which was also used for the localization of the transition states. Frequency analyses at the same theory level were performed to confirm that all structures correspond to minima or transition states. The thermochemical corrections G_{corr} obtained in that way were next combined with single point energies $E_{tot,\ Def2\text{-}TZVP}$ at the SMD(DCM)/MN15/def2-TZVP[28] level to afford the Gibbs energies $G^{298}_{Def2\text{-}TZVP}$. Finally, Gibbs energies $G^{298}_{Def2\text{-}TZVP}$ for different conformations were Boltzmann weighted and a free energy change of +7.91 kJ/mol (= R · 298 K · ln(22.46 L mol^{-1}/L mol^{-1})) was applied for their conversion from gas phase (1 atm) to liquid phase (1 M). See Supporting Information for the geometries of all optimized structures.

Acknowledgements

[1] F. Effenberger, *Acc. Chem. Res.* **1989**, *22*, 27-35.

[2] a) J. L. Segura, N. Martin, *Angew. Chem.* **2001**, *113*, 1416-1455; *Angew. Chem. Int. Ed.* **2001**, *40*, 1372–1409; b) for a conversion calculator of redox potentials measured toward different reference electrodes: http://www.consultrsr.net/resources/ref/refpotls3.htm (accessed on July 2021); c) for solvent dependence of electrochemical references: J. Ruiz Aranzaes, M.-C. Daniel, D. Astruc, *Can. J. Chem.* **2006**, *84*, 288-299.

[3] a) W. Knoche, W. W. Schoeller, R. Schomäcker, S. Vogel, *J. Am. Chem. Soc.*, **1988**, *110*, 7484-7489; b) W. Sachs, W. Knoche, C. Herrmann, *J. Chem. Soc., Perkin Trans. 2* **1991**, 701-710.

[4] a) C. Boga, E. Del Vecchio, L. Forlani, A. Mazzanti, P. E. Todesco, *Angew. Chem.* **2005**, *117*, 3349–3353; *Angew. Chem. Int. Ed.* **2005**, *44*, 3285–3289; b) C. Boga, E. Del Vecchio, L. Forlani, A. Mazzanti, C. Menchen Lario, P. E. Todesco, S. Tozzi, *J. Org. Chem.* **2009**, *74*, 5568–5575; c) C. Boga, G. Micheletti, S. Cino, S. Fazzini, L. Forlani, N. Zanna, D. Spinelli, *Org. Biomol. Chem.* **2016**, *14*, 4267-4275.

[5] J. Hine, R. D. Weimar Jr., *J. Am. Chem. Soc.* **1965**, *87*, 3387−3396.

[6] H. Mayr, J. Ammer, M. Baidya, B. Maji, T. A. Nigst, A. R. Ofial, T. Singer, *J. Am. Chem. Soc.* **2015**, *137*, 2580-2599.

[7] a) H. Mayr, T. Bug, M. F. Gotta, N. Hering, B. Irrgang, B. Janker, B. Kempf, R. Loos, A. R. Ofial, G. Remennikov, H. Schimmel, *J. Am. Chem. Soc.* **2001**, *123*, 9500-9512; b) H. Mayr, *Angew. Chem.* **2011**, 123, 3692-3698; *Angew. Chem. Int. Ed.* **2011**, *50*, 3612-3618; c) H. Mayr, *Tetrahedron* **2015**, *71*, 5095-5111; d) A database of reactivity parameters

[8] E, N, and s_N is freely accessible through the webpage www.cup.lmu.de/oc/mayr/DBintro.html (accessed on June 2021).

[8] International Union of Pure and Applied Chemistry (IUPAC), Compendium of Chemical Terminology, 2nd Ed., 2019.

[9] a) H. Mayr, A. R. Ofial, *Acc. Chem. Res.* **2016**, *49*, 952-965; b) E. Follet, H. Zipse, S. Lakhdar, A. R. Ofial, G. Berionni, *Synthesis* **2017**, *49*, 3495-3504; c) E. Follet, P. Mayer, D. S. Stephenson, A. R. Ofial, G. Berionni, *Chem. Eur. J.* **2017**, *23*, 7422-7427; d) R. J. Mayer, M. Breugst, N. Hampel, A. R. Ofial, H. Mayr, *J. Org. Chem.* **2019**, *84*, 8837-8858.

[10] D. S. Timofeeva, R. J. Mayer, P. Mayer, A. R. Ofial, H. Mayr, *Chem. Eur. J.* **2018**, *24*, 5901-5910.

[11] G. Micheletti, C. Boga, *Synthesis* **2017**, *49*, 3347-3356.

[12] V. V. Negrebetskii, N. N. Bichkov, B. I. Stepanov, *J. Gen. Chem USSR* (Engl. Transl.) **1980**, *50*, 1658-1662.

[13] J. Ammer, C. F. Sailer, E. Riedle, H. Mayr, *J. Am. Chem. Soc.* **2012**, *134*, 11481-11494.

[14] B. Maji, X.-H. Duan, P. M. Jüstel, P. A. Byrne, A. R. Ofial, H. Mayr, *Chem. Eur. J.* **2021**, *27*, 11367–11376.

[15] a) D. N. Kevill, S. W. Anderson, N. H. Ismail, *J. Org. Chem.* **1996**, *61*, 7256-7262; b) M. Matić, B. Denegri, S. Jurić, O. Kronja, *Croat. Chem. Acta* **2017**, *90*, 571-581; c) B. Denegri, M. Matić, O. Kronja, *Synthesis* 2017, 49, 3422-3432.

[16] H. Eyring, *Chem. Rev.* **1935**, *17*, 65–77.

[17] a) R. Niess, K. Nagel, F. Effenberger, *Tetrahedron Lett.* **1968**, 4265-4268; b) F. Effenberger, K. E. Mack, K. Nagel, R. Niess, *Chem. Ber.* **1977**, *110*, 165-180.

[18] C. Boga, L. Forlani, S. Tozzi, E. Del Vecchio, A. Mazzanti, M. Monari, N. Zanna, *Curr. Org. Chem.* **2014**, *18*, 512-523.

[19] S. Lakhdar, M. Westermaier, F. Terrier, R. Goumont, T. Boubaker, A. R. Ofial, H. Mayr, *J. Org. Chem.* **2006**, *71*, 9088-9095.

[20] J. H. Brown, C. H. Bushweller, QCPE Bulletin: Bloomington, IN, **1983**, *3*, 103–103.

[21] R. J. Mayer, N. Hampel, P. Mayer, A. R. Ofial, H. Mayr, *Eur. J. Org. Chem.* **2019**, 412-421.

[22] S. Cino, PhD Thesis, University of Bologna, 2016, http://amsdottorato.unibo.it/7566/.

[23] E. Harder, W. Damm, J. Maple, C. Wu, M. Reboul, J. Y. Xiang, L. Wang, D. Lupyan, M. K. Dahlgren, J. L. Knight, J. W. Kaus, D. S. Cerutti, G. Krilov, W. L. Jorgensen, R. Abel, R. A. Friesner, *J. Chem. Theory Comput.* **2016**, *12*, 281-296.

[24] Schrödinger Release 2019-4: MacroModel, Schrödinger, LLC, New York, NY, 2019.

[25] Gaussian 16, Revision A.03, M. J. Frisch, G. W. Trucks, H. B. Schlegel, G. E. Scuseria, M. A. Robb, J. R. Cheeseman, G. Scalmani, V. Barone, G. A. Petersson, H. Nakatsuji, X. Li, M. Caricato, A. V. Marenich, J. Bloino, B. G. Janesko, R. Gomperts, B. Mennucci, H. P. Hratchian, J. V. Ortiz, A. F. Izmaylov, J. L. Sonnenberg, D. Williams-Young, F. Ding, F. Lipparini, F. Egidi, J. Goings, B. Peng, A. Petrone, T. Henderson, D. Ranasinghe, V. G. Zakrzewski, J. Gao, N. Rega, G. Zheng, W. Liang, M. Hada, M. Ehara, K. Toyota, R. Fukuda, J. Hasegawa, M. Ishida, T. Nakajima, Y. Honda, O. Kitao, H. Nakai, T. Vreven, K. Throssell, J. A. Montgomery Jr., J. E. Peralta, F. Ogliaro, M. J. Bearpark, J. J. Heyd, E. N. Brothers, K. N. Kudin, V. N. Staroverov, T. A. Keith, R. Kobayashi, J. Normand, K. Raghavachari, A. P. Rendell, J. C. Burant, S. S. Iyengar, J. Tomasi, M. Cossi, J. M. Millam, M. Klene, C. Adamo, R. Cammi, J. W. Ochterski, R. L. Martin, K. Morokuma, O. Farkas, J. B. Foresman, D. J. Fox, Gaussian, Inc., Wallingford CT, 2016.

[26] A. V. Marenich, C. J. Cramer, D. G. Truhlar, *J. Phys. Chem. B* **2009**, *113*, 6378-6396.

[27] H. S. Yu, X. He, S. L. Li, D. G. Truhlar, *Chem. Sci.* **2016**, *7*, 5032-5051.

[28] F. Weigend, R. Ahlrichs, *Phys. Chem. Chem. Phys.* **2005**, *7*, 3297-3305.

11

FULL PAPER

Entry for the Table of Contents
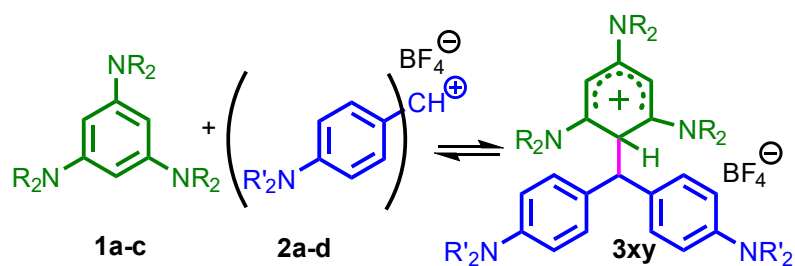
Equilibrium constants for the formation of **3xy** have been determined photometrically. The Lewis basicity of the ring carbons trend is: trimorpholinobenzene **1a** < tripiperidinobenzene **1b** < tripyrrolidinobenzene **1c**; nucleophilicity parameters are in the range $10 < N < 15$. Some complexes show temperature-dependent NMR spectra, due to rapid reverse reaction and recombination at different positions of the ring. DFT calculations agree with experimental data.